Comparison of the Performance of the VSI-Fed Adjustable-Speed Drives Under Balanced and Unbalanced Voltage Sag Conditions

M. Abou El-Azaim Mahdy, A. F. Zobaa, *Senior Member, IEEE*, and M. M. Abdel Aziz, *Senior Member, IEEE*

***Abstract*— Adjustable-Speed Drives are one of the most sensitive equipments to voltage sags. Even though there have been numerous studies addressing Adjustable-Speed Drives effects on power systems, models for predicting the effect of the source voltage sags or unbalance have been limited. In this paper a comparison between different models of the ac motor and inverter of Adjustable-Speed Drives during balanced and unbalanced voltage sag conditions is studied using MATLAB/Simulink.**

***Keywords*–** Adjustable-Speed Drive (ASD), Power Quality and Voltage Sag

I. INTRODUCTION

Most of the modern loads whether on the industrial or commercial scales are inverter-based such as Adjustable-Speed Drives (ASDs), Voltage/Frequency Controlled Power Supplies etc, due to their improved efficiency, energy saving, and high controllability. However, the ASDs are often susceptible to the electric power disturbances that sometimes take place in the grid such as sags, swells, transients and momentary interruptions [1]. This might lead the ASD to trip depending on the nature and the severity of the disturbance. Such trips causes sever financial losses if the ASD is driving a critical process.

The most frequent disturbance is the Voltage Sag (about 70% of the registered disturbances [2]) that is defined as a momentary decrease in the root mean square voltage between 10% to 90%, with a duration ranging from half cycle up to 1 min [3,4]. According to survey reports, voltage of 10% - 30% below nominal for 3-30 cycle durations account for the majority of power system disturbances, and are the major cause of industry process disruptions [1].

Different reasons lead to voltage sags. They can be due to fault conditions within the plant or power system or on the utility scale due to lightning, wind, contamination of insulators, animals or accidents [5]. Sags due to these reasonslast until the fault ends or the fault are cleared by a fuse or breaker.

M. Abou El-Azaim Mahdy is with Middle Egypt Co. for Electricity Distribution, Benisuef, Egypt (e-mail: azaim2000@ yahoo.com).

A. F. Zobaa and M. M. Abdel Aziz are with Electrical Power & Machines Dept, Faculty of Engineering, Cairo University, Giza, 12613, Egypt.

Large motors startups or connecting large loads to the grid in an area close to the ASD or even at the same plant are also potential reasons for voltage sags.

Disrupting a critical process in continuous process systems can result in a significant loss in revenue and costly downtime. According to estimations; the cumulative losses due to power disturbances in the U.S. range from $20 billion to $100 billion per year. According to industrial reports, the range of losses per disrupting event range from $10,000 to $1 million [1].

Due to the high economical losses of the production loss caused by tripping out of ASDs, it's very important to study different approaches that can improve the ridethrough capabilities of ASDs to voltage sags.

In order to analyze in detail the performance of ASDs under input voltage unbalance and sag conditions the inverter and the ac motor can be modeled as a constant current source [7], [8],[11] and [12] or a resistance [13] -[17], or a constant power load [2] and [18], or A complex model [9]

In this paper a comparison of the performance of ASDs using the previous models of the ac motor and inverter during balanced and unbalanced voltage sag conditions is studied, using Matlab/Simulink.

II. BASIC CONSTRUCTION OF ADJUSTABLE SPEED DRIVES

An ASD controls the speed of an induction or synchronous motor by converting fixed frequency/fixed magnitude ac mains supply voltage to a variable frequency/variable magnitude voltage at the motor terminals. The dominant type of ASD in several hundreds up to the megawatt range is the pulse-width-modulation (PWM)-controlled voltage-source inverter.

ASDs are widely used in modern processes. Improved process control, high dynamic performance, increased flexibility, energy savings in applications with variable torque loads and reduced motor speeds, reduction of mechanical and thermal stresses through “soft” start, acceleration, and deceleration, remote communication and control, simple maintenance and automated diagnostic are some of the benefits which ASDs provide and driving the ASD's market. On the other hand, reliable operation of these ASD’s has to be guaranteed in order to avoid malfunctioning or interruption of the process

Fig. 1, shows a typical ASD topology, which consists of a rectifier, a direct current link, and an inverter. The rectifier

converts supply AC voltage into a DC voltage. The DC voltage is filtered by the DC link capacitor.

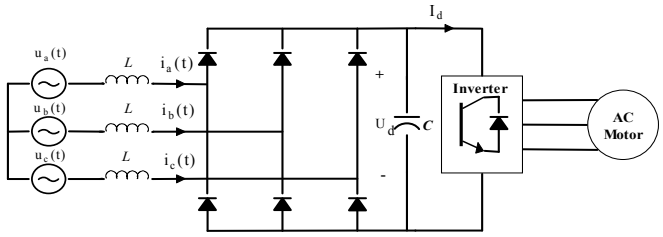

Fig. 1. Typical VSI-fed ASD topology

The inverter converts the DC to an adjustable frequency, adjustable voltage AC for motor speed control.

Due to the advantageous properties of voltage-source-inverter (VSI)-fed drives, such as low starting currents and significant energy savings, especially in pump and fan applications, such drives are frequently used nowadays.

V. CHARACTERIZATION AND CLASSIFICATION OF VOLTAGE SAGS

Voltage sags are widely recognized as one of the most important aspects of power quality. Large power quality surveys have been performed in several countries. Analysis of the results requires a definition and understanding of various voltage sag characteristics.

Magnitude and duration are the main characteristics of voltage sags, and they have been used for the development of the equipment's compatibility charts and indices. In addition to these, the other characteristics such as unbalanced voltage sags, phase angle shifts, the initial point on wave and waveform distortion have been found to influence significantly the equipment's sensitivity to voltage sags [5].

In this paper the voltage sag characteristics which have been considered are; the sag depth (h), duration (Δt) and initial point on wave (ψi) because they have the greatest influence on the equipment sensitivity to voltage sags.

Voltage sags can be classified based on the type of fault which causes the voltage sag, to [1]:

- Unbalanced voltage sags:
  - Voltage sags due to single-phase to ground faults (SLGF) (Includes types B, C* and D* sags);
  - Voltage sags due to phase-to-phase faults (LLF) (Includes types C and D sags);
  - Voltage sags due to two-phase-to-ground faults (LLGF) (Include types E, F and G sags).
- Balanced voltage sags (Includes type A sag).

The characteristic equations for the four types, which will be studied in this paper, are as follow [1]:

Type B sag:

$$U_a = hU$$

$$U_b = -\frac{1}{2}U - j\frac{\sqrt{3}}{2}U \qquad (1)$$

$$U_c = -\frac{1}{2}U + j\frac{\sqrt{3}}{2}U$$

Type C sag:

$$U_a = U$$

$$U_b = -\frac{1}{2}U - j\frac{\sqrt{3}}{2}hU \qquad (2)$$

$$U_c = -\frac{1}{2}U + j\frac{\sqrt{3}}{2}hU$$

Type F sag:

$$U_a = hU$$

$$U_b = -\frac{1}{2}hU - j\frac{1}{\sqrt{12}}(2+h)U \qquad (3)$$

$$U_c = -\frac{1}{2}hU + j\frac{1}{\sqrt{12}}(2+h)U$$

Type A sag:

$$U_a = hU$$

$$U_b = -\frac{1}{2}hU - j\frac{\sqrt{3}}{2}hU \qquad (4)$$

$$U_c = -\frac{1}{2}hU + j\frac{\sqrt{3}}{2}hU$$

Where h=0-1, $U_{a,}$ U_b and U_c are the phase to neutral voltages in case of a voltage sag condition and U is the peak value of the input voltage in case of normal operation

VI. MODELING OF VSI-FED ADJUSTABLE SPEED DRIVES

Development of ASDs relies mainly on simulation techniques which depend heavily on adequate models of the drive and a good understanding of the sensitivities of the models with respect to the data available for model construction. It was also important to be able to predict the drive's behavior in different conditions to investigate with high-quality simulations rapidly any problem occurring and hardly measurable [6].

The remarkable reduction in computing time makes the models very attractive for analyses that need a very high number of simulations.

The most widely used method to analyze the performance of ASDs under input voltage unbalance and sag conditions is the time-domain simulation by means of simulation tools like P-Spice [7], [8], Matlab/Simulink [9], [10].

In order to analyze in detail the performance of ASDs under input voltage unbalance and sag conditions the inverter and the ac motor can be modeled as:

- A constant current source;
- A resistance;
- A constant power load;
- A complex model

A. Constant Current Source Model

The inverter and ac motor can be modeled as a constant current source as in [7], [8], [11] and [12].

Reference [12] shows that there is little need to model the current source as a harmonic source because the inverter harmonics are negligible as seen from the converter AC side.

This is because, in the case of PWM and VSI type ASDs, the inverter harmonics are largely bypassed by the DC link capacitor before they can penetrate into the supply system side. In the case of CSI type ASD, the series inductor serves as a large impedance to block inverter harmonics from ever getting into the converter.

B. Resistance Model

When the ac voltage generated by the inverter changes, the induction motor can be considered as a constant impedance (a constant resistance viewed from the dc side of the ASD) [13], [14], [15] and [16]. The interaction between supply-side and motor-side signal frequencies can be assumed as negligible in analyzing the effects of the supplying voltage distortion and, then, the resistor R absorbs the same dc-current component of the inverter-motor group [17].

C. Constant Power Load Model

In [2] and [18] it was assumed that the input power to the ASD is constant during normal and voltage sag conditions. In [7] it was stated that if the speed of ac motor changes, the motor can be considered as a constant power load and this model is adequate for long-time perturbations.

D. Complex model

In [9] the input current to the inverter was calculated by assuming that input and output instantaneous powers are equal and the induction motor was modeled by the 5th-order Park equations**.** Euler's method has been used for solving the differential equations.

VII. SIMULATED RESULTS AND DISCUSSION

Assuming that the average dc voltage in steady-state U_d is approximately the dc voltage of a rectifier with infinite dc inductance and no inductance on the ac side (ideal rectifier).

$$U_d = \frac{3\sqrt{2}}{\pi} U_L = 1.35\, U_L \quad (5)$$

Where U_L is the rms ac line voltage.

The output voltage of an ideal 3-ph PWM inverter $u_{ac,inv}$ can be calculated from [19]:

$$u_{ac,inv} = \frac{\sqrt{3}}{2\sqrt{2}} * m * U_d \quad (6)$$

Where m is the modulation index =1.

The dc-side electrical power P_d is determined by the mechanical power P_m, the VSI efficiency η_{VSI} and the mechanical efficiency η_m [7].

$$P_d = P_m / (\eta_m \eta_{VSI}) \quad (7)$$

And from the given motor data it can also be calculated through the dc voltage and current U_d and I_d

$$P_d = U_d I_d \quad (8)$$

The simulated induction motor used in this paper is used as a slandered model in Matlab/Simulink and has the following parameters: P_m=50hp, U_L=460V, frequency f =60 Hz, rotor speed N=1780rpm, rated shaft mechanical torque Tm=200N.m and η_m=82.3%.An ideal inverter is considered hence VSI efficiency η_{VSI} =1

From (6), when $u_{ac,inv}$=460V then U_d =751V, and from (5): U_L = 454.2V.

From the given motor data and from (7):
P_d = 50hp x 746 /(0.823 x 1) = 45.322 kw.

From (8) if U_d =751V then I_d = 45322/751=60.35A.

Typical values for L and C are taken from [7], the intermediate values are L=0.66mH, C=3mF.

From the previous discussion the inverter and induction motor can be modeled as:

- Resistance with $R=U_d / I_d$ = 751/60.35 = 12.44 ohm.
- Constant current source with I_d = 60.35A.
- Constant power load with Pd=45.322 kw.
- Complex model consists of an ideal inverter and the Matlab/Simulink model of the previously discussed induction motor.

A. Comparison between Different Models

The comparison of the performance of the VSI-Fed ASDs under voltage sag conditions is studied using two variables that may cause ASD to trip. These variables are the minimum dc voltage during the sag U_{dmin} (pu) and the maximum ac current peak i_{max} produced by the sag. The per-unit values of the two variables can be calculated from (9) and (10).

$$U_{d\,min}(pu) = U_{d\,min} / 1.35U_L = min\{U_d(t)\} / 1.35U_L \quad (9)$$

$$i_{max}(pu) = i_{max} / I_d = max\{|i_a(t)|, |i_b(t)|, |i_c(t)|\} / I_d \quad (10)$$

The influence of the ac motor and inverter model on the behaviour of ASDs during four types of voltage sags (Types B, C, F and A) is studied in this paper using Matlab/Simulink analysis. The current source model, the resistance model and the constant power load model are compared with the complex model.

The relative error for all models is calculated in all the studied cases, taking the complex model as the reference model, from (11),(12) and (13).

$$\Delta E_i = \left| \frac{i_{max,\ complex}\ (pu) - i_{max,\ mod}\ (pu)}{i_{max,\ complex}\ (pu)} \right| \times 100 \quad (11)$$

$$\Delta E_u = \left| \frac{u_{d\,min,\ complex}\ (pu) - u_{d\,min,\ mod}\ (pu)}{u_{d\,min,\ complex}\ (pu)} \right| \times 100 \quad (12)$$

$$\Delta E_{total} = \Delta E_i + \Delta E_U \quad (13)$$

Where:

$i_{max,complex}$: the maximum input current in case of the complex model,

$i_{max,mod}$: the maximum input current in case of any other model,

$u_{dmin,complex}$: the minimum dc output voltage in case of the complex model,

$u_{dmin,mod}$: the minimum dc output voltage in case of any other model,

ΔE_i: the relative error for i_{max}(pu),
ΔE_U: the relative error for U_{dmin}(pu) and
ΔE_{total}: the total relative error.

B. Comparison during Type B sag

Table I shows a comparison of the four models of inverter and induction motor for type B sag at (h=0.25, 0.5 and 0.75 and Δt=1cycle (1T), 5, 10 and 20T).

Table I
Models Comparison during Type B sag

Type B		Δt =1T					Δt =5T					Δt =10T					Δt =20T				
		i_{max} pu	ΔE_i %	U_{dmin} pu	ΔE_U %	ΔE_{total} %	i_{max} pu	ΔE_i %	U_{dmin} pu	ΔE_U %	ΔE_{total} %	i_{max} pu	ΔE_i %	U_{dmin} pu	ΔE_U %	ΔE_{total} %	i_{max} pu	ΔE_i %	U_{dmin} pu	ΔE_U %	ΔE_{total} %
h=0.25	R	3.39	9.8	0.85	2.4	12.2	3.39	9.8	0.85	2.4	12.2	3.39	9.8	0.85	2.4	12.2	3.39	9.8	0.85	2.4	12.2
	CS	3.71	1.3	0.84	1.2	2.5	3.71	1.3	0.84	1.2	2.5	3.71	1.3	0.84	1.2	2.5	3.71	1.3	0.84	1.2	2.5
	Const.P	4.13	9.8	0.82	1.2	11	4.13	9.8	0.82	1.2	11	4.13	9.8	0.82	1.2	11	4.13	9.8	0.82	1.2	11
	Complex	3.76	-	0.83	-	-	3.76	-	0.83	-	-	3.76	-	0.83	-	-	3.76	-	0.83	-	-
h=0. 5	R	3.39	9.8	0.85	2.4	12.2	3.39	9.8	0.85	2.4	12.2	3.39	9.8	0.85	2.4	12.2	3.39	9.8	0.85	2.4	12.2
	CS	3.71	1.3	0.84	1.2	2.5	3.71	1.3	0.84	1.2	2.5	3.71	1.3	0.84	1.2	2.5	3.71	1.3	0.84	1.2	2.5
	Const.P	4.13	9.8	0.82	1.2	11	4.13	9.8	0.82	1.2	11	4.13	9.8	0.82	1.2	11	4.13	9.8	0.82	1.2	11
	Complex	3.76	-	0.83	-	-	3.76	-	0.83	-	-	3.76	-	0.83	-	-	3.76	-	0.83	-	-
h=0.75	R	3.28	8.4	0.86	2.4	10.8	3.28	8.4	0.86	2.4	10.8	3.28	8.4	0.86	2.4	10.8	3.28	8.4	0.86	2.4	10.8
	CS	3.53	1.4	0.85	1.2	2.6	3.53	1.4	0.85	1.2	2.6	3.53	1.4	0.85	1.2	2.6	3.53	1.4	0.85	1.2	2.6
	Const.P	3.86	7.8	0.84	0	7.8	3.86	7.8	0.84	0	7.8	3.86	7.8	0.84	0	7.8	3.86	7.8	0.84	0	7.8
	Complex	3.58	-	0.84	-	-	3.58	-	0.84	-	-	3.58	-	0.84	-	-	3.58	-	0.84	-	-

From Table I, it can be seen that during type B sag, in all the studied cases, ΔE_{total} is minimum in case of the current source model. So we can say that the current source model is the most accurate model in case of type B sag.

C. Comparison during Type C sag

Table II shows a comparison of the four models of inverter and induction motor for type C sag at (Δt=1, 5, 10 and 20T and h=0.25, 0.5and 0.75).

Table II
MODELS COMPARISON DURING TYPE C SAG

Type C		Δt =1T					Δt =5T					Δt =10T					Δt =20T				
		i_{max} pu	ΔE_i %	U_{dmin} pu	ΔE_U %	ΔE_{total} %	i_{max} pu	ΔE_i %	U_{dmin} pu	ΔE_U %	ΔE_{total} %	i_{max} pu	ΔE_i %	U_{dmin} pu	ΔE_U %	ΔE_{total} %	i_{max} pu	ΔE_i %	U_{dmin} pu	ΔE_U %	ΔE_{total} %
h=0.25	R	3.55	21	0.75	5	26	3.55	20	0.75	5.6	25.6	3.55	20	0.75	5.6	25.6	3.55	20	0.75	5.6	25.6
	CS	4.43	1.5	0.72	9	10.5	4.43	0	0.72	1.4	1.4	4.43	0	0.72	1.4	1.4	4.43	0	0.72	1.4	1.4
	Const.P	5.85	30	0.67	15.2	45.2	5.85	32	0.67	5.6	37.6	5.85	32	0.67	5.6	37.6	5.85	32	0.67	5.6	37.6
	Complex	4.5	-	0.79	-	-	4.43	-	0.71	-	-	4.43	-	0.71	-	-	4.43	-	0.71	-	-
h=0.5	R	3.01	24	0.78	5	29	3.01	16.8	0.78	2.6	19.4	3.01	16.8	0.78	2.6	19.4	3.01	16.8	0.78	2.6	19.4
	CS	3.61	8.8	0.77	6	14.8	3.61	0.3	0.77	1.3	1.6	3.61	0.3	0.77	1.3	1.6	3.61	0.3	0.77	1.3	1.6
	Const.P	4.49	13.4	0.74	9.8	23.2	4.49	24	0.74	2.6	26.6	4.49	24	0.74	2.6	26.6	4.49	24	0.74	2.6	26.6
	Complex	3.96	-	0.82	-	-	3.62	-	0.76	-	-	3.62	-	0.76	-	-	3.62	-	0.76	-	-
h=0.75	R	2.3	23.3	0.85	1.1	24.4	2.35	9	0.85	2.4	11.4	2.35	9	0.85	2.4	11.4	2.35	9	0.85	2.4	11.4
	CS	2.58	14	0.84	2.3	16.3	2.58	0	0.84	1.2	1.2	2.58	0	0.84	1.2	1.2	2.58	0	0.84	1.2	1.2
	Const.P	2.97	1	0.83	3.5	4.5	2.97	15	0.83	0	15	2.97	15	0.83	0	15	2.97	15	0.83	0	15
	Complex	3	-	0.86	-	-	2.58	-	0.83	-	-	2.58	-	0.83	-	-	2.58	-	0.83	-	-

From Table II it can be shown that during type C sag the constant power load model is the most accurate in only one case at (Δt=1T and h=0.75) and the current source model is the most accurate model in the other eleven cases. So we can say that the current source model is the most accurate mode during type C sag.

D. Comparison during Type F sag

Table III shows a comparison of the four models of inverter and induction motor for type F sag at (Δt=1 and 5T and h=0.5, 0.65and 0.75)

Table III
MODELS COMPARISON DURING TYPE F SAG

Type F		Δt =1T					Δt =5T					Δt =10T					Δt =20T				
		i_{max} pu	ΔE_i %	U_{dmin} pu	ΔE_U %	ΔE_{total} %	i_{max} pu	ΔE_i %	U_{dmin} pu	ΔE_U %	ΔE_{total} %	i_{max} pu	ΔE_i %	U_{dmin} pu	ΔE_U %	ΔE_{total} %	i_{max} pu	ΔE_i %	U_{dmin} pu	ΔE_U %	ΔE_{total} %
h=0.5	R	5.48	7	0.69	3	10	4.99	10	0.69	10	20	4.99	17.5	0.69	9.5	27	4.99	17.5	0.69	9.5	27
	CS	6.49	27	0.66	7	34	5.73	3	0.66	5	8	5.7	5.8	0.66	4.8	10.6	5.7	5.8	0.66	4.8	10.6
	Const.P	8.15	59.8	0.6	16	75.8	7.72	38.9	0.6	5	43.9	7.32	21	0.6	4.8	25.8	6.36	5.1	0.6	4.8	9.9
	Complex	5.1	-	0.71	-	-	5.56	-	0.63	-	-	6.05	-	0.63	-	-	6.05	-	0.63	-	-
h=0.65	R	4.7	2.1	0.74	0	2.1	4.32	6.1	0.74	7.2	13.3	4.32	12.7	0.74	7.2	19.7	4.32	14.5	0.74	7.2	21.7
	CS	5.4	12.5	0.72	2.7	15.2	4.89	6.3	0.72	4	10.3	4.86	1.8	0.72	4.3	6.1	4.86	3.8	0.72	4.3	8.1
	Const.P	6.3	31.2	0.69	6.8	38	5.9	28	0.69	0	28	5.45	10	0.69	0	10	5.15	2	0.69	0	2
	Complex	4.8	-	0.74	-	-	4.6	-	0.69	-	-	4.95	-	0.69	-	-	5.05	-	0.69	-	-
h=0.75	R	4.04	9	0.78	1	10	3.86	5	0.78	4	9	3.86	9.6	0.78	4	13.6	3.86	11	0.78	4	15
	CS	4.42	0	0.78	1	1	4.26	5	0.77	3	8	4.24	0.7	0.77	2.67	3.37	4.24	2.3	0.77	2.67	4.97
	Const.P	4.87	10	0.76	1	11	4.77	17	0.76	1	18	4.76	11.5	0.76	1.33	12.83	4.76	9.7	0.76	1.33	11.03
	Complex	4.42	-	0.77	-	-	4.07	-	0.75	-		4.27	-	0.75	-	-	4.34	-	0.75	-	-

From Table III it can be shown that during type F sag, ΔE_{total} is minimum in case of the current source model in eight cases from the studied twelve cases. So the current source model is the most accurate model during type F sag.

E. Comparison during Type A sag

Table IV shows a comparison of the four models of inverter and induction motor for type A sag at (Δt=1,5,10,20T and h=0.5, 0.65and 0.75).

Table IV
MODELS COMPARISON DURING TYPE A SAG

Type A		Δt =1T					Δt =5T					Δt =10T					Δt =20T				
		i_{max} pu	ΔE_i %	U_{dmin} pu	ΔE_U %	ΔE_{total} %	i_{max} pu	ΔE_i %	U_{dmin} pu	ΔE_U %	ΔE_{total} %	i_{max} pu	ΔE_i %	U_{dmin} pu	ΔE_U %	ΔE_{total} %	i_{max} pu	ΔE_i %	U_{dmin} pu	ΔE_U %	ΔE_{total} %
h=0.5	R	6.36	19	0.62	8.8	27.8	9.14	16	0.47	6.8	22.8	9.14	15.4	0.47	6.8	22.2	9.14	11.9	0.47	6.8	18.7
	CS	8.58	60	0.53	22	82	9.8	10	0.45	2.8	12.8	9.8	9.3	0.45	2.3	11.6	9.8	5.5	0.45	2.3	7.8
	Const.P	13.39	150	0.37	45.6	195.6	11.4	5	0.36	18.2	23.2	11.13	3	0.36	18.2	21.2	11.13	7.3	0.36	18.2	25.5
	Complex	5.35	-	0.68	-	-	10.9	-	0.44	-	-	10.8	-	0.44	-	-	10.37	-	0.44	-	-
h=0. 65	R	6.33	18	0.63	8.7	26.7	6.33	12	0.62	5.1	17.1	6.33	15.5	0.62	5.1	20.6	6.33	14.7	0.62	5.1	19.8
	CS	7.36	37.5	0.6	13	50.5	6.79	6	0.6	1.7	7.7	6.79	9.3	0.6	1.7	11	6.79	8.5	0.6	1.7	10.2
	Const.P	7.57	41.5	0.56	18.8	60.3	7.57	5	0.56	5	10	7.57	1	0.56	3	4	7.57	2	0.56	3	5
	Complex	5.35	-	0.69	-	-	7.22	-	0.59	-	-	7.49	-	0.59	-	-	7.42	-	0.59	-	-
h=0.75	R	4.64	6.6	0.71	0	6.6	4.54	7.7	0.71	1.4	9.1	4.54	12.5	0.71	1.4	13.9	4.54	12.7	0.71	1.4	14.1
	CS	4.72	5	0.7	1.4	6.4	4.89	0.6	0.7	0	0.6	4.89	5.8	0.7	0	5.8	4.89	6	0.7	0	6
	Const.P	4.82	3	0.67	5.6	8.6	5.38	9.3	0.67	4.3	13.6	5.4	4	0.67	4.3	8.3	5.4	3.8	0.67	4.3	8.1
	Complex	4.97	-	0.71	-	-	4.92	-	0.7	-	-	5.19	-	0.7	-	-	5.2	-	0.7	-	-

From Table IV it can be seen that during type A sag, ΔE_{total} is minimum in case of the current source model in eight cases from the studied twelve cases. So the current source model is the most accurate model during type A sag.

VIII. CONCLUSION

In this paper the effect of different types of voltage sags on the minimum dc voltage drop and the maximum ac current peaks on ASDs using four models of induction motor and inverter was studied.

The comparison between the resistance, the current source, the constant power load and the complex models, which was taken as the reference model, concludes that:

In case of type B voltage sag which is caused by single-phase to ground faults, which are the most frequent sags (80% of the sags), the current source model is the most accurate model in all of the studied cases

In case of voltage sags caused by line-to-line faults (type C), voltage sags caused by two-phase-to-ground faults (type F) and voltage sags caused by three phase faults (type A) the current source model is the most accurate model in the majority of the studied cases.

In all of the studied cases the current source model gives intermediate results between the resistance and constant power load models.

From the previous conclusions the current source model can be considered as the most accurate model of inverter and induction motor of VSI-fed ASDs during balanced and unbalanced voltage sags.

REFERENCES

[1] M. H. J. Bollen, Understanding Power Quality Problems: Voltage Sags and Interruptions, IEEE Press Series on Power Engineering. IEEE Press, 2000.

[2] M. H. J. Bollen and L. D. Zhang, “Analysis of voltage tolerance of AC adjustable-speed drives for three-phase balanced and unbalanced sags,” IEEE Trans. Ind. Applicat., vol. 36, no. 3, pp. 904–910, May/Jun. 2000.

[3] M. McGranaghan, D. R. Mueller, and M. Samotyj, “Voltage sag in industrial systems,” IEEE Trans. Ind. Appl., vol. 29, no. 2, pp. 397–403, Mar./Apr. 1993.

[4] J. V. Milanovic, R. Gnativ, and K. W. M. Chow, “The influence of loading conditions and network topology on voltage sags,” in Proc. Ninth Int. Conf. Harmonics Quality Power, vol. 2, Oct. 1–4, 2000, pp. 757–762.

[5] R. Gnativ and J. V. Milanovi, “Voltage sag propagation in systems with embedded generation and induction motors,” in Proc. IEEE Power Engineering Society Summer Meeting, vol. 1, Jul. 15–19, 2001, pp. 474–479.

[6] Alain Sapin, Peter K. Steimer and Jean-Jacques Simond," Modeling, Simulation, and Test of a Three-Level Voltage-Source Inverter With Output LC Filter and Direct Torque Control " IEEE Trans. Ind. Applicat., vol, 43, no. 2, pp. 469–475, Mar/Apr. 2007

[7] J. Pedra, F. Córcoles, and F. J. Suelves "Effects of Balanced and Unbalanced Voltage Sags on VSI-Fed Adjustable-Speed Drives". IEEE Trans. Power Delivery. Vol. 20, No. 1, Jan. 2005.

[8] M. Grotzbach and R. Redmann, “Line current harmonics of VSI-fed adjustable-speed drives,” *IEEE Trans. Ind. Applicat*., vol. 36, no. 2, pp. 683–690, Mar./Apr. 2000.

[9] M. H. J. Bollen and R. A. A. De Graaff, “Behavior of AC and DC drives during voltage sags with phase-angle jump and three-phase unbalance,” in *IEEE Power Eng. Soc. Winter Meeting*, vol. 2, New York, Jan./Feb. 1999, pp. 1225–1230.

[10] Yong-Seok Kim and Seung-Ki Sul,"A Novel Ride-Through System for Adjustable-Speed Drives Using Common-Mode Voltage", *IEEE Trans. Ind. Applicat*, vol. 37, no. 5, pp.1373-1382,Sept/Oct.2001.

[11] Wilsun Xu, Hermann W. Dommel, M. Brent Hughes, Gay W.K. Chang and Le Tan" Modelling of Adjustable Speed Drives for Power System Harmonic Analysis",*IEEE Trans. Power Delivery*, vol. 14, no. 2, pp. 595-601,April 1999.

[12] W. Xu, H.W. Dommel, M. B. Hughes, G.W. Chang, and L. Tan, “Modeling of adjustable speed drives for power system harmonic analysis,” IEEE Trans. Power Delivery., vol. 14, no. 2, pp. 595–601, Apr. 1999.

[13] K. Stockman, F. D’hulster, K. Verhaege, M. Didden, and R. Belmans, “Ride-through of adjustable speed drives during voltage dips,” Elect. Power Syst. Res., vol. 66, pp. 49–58, Jul. 2003.

[14] Kevin Lee, Thomas M. Jahns, Giri Venkataramanan, and William E. Berkopec, " DC-Bus Electrolytic Capacitor Stress in Adjustable-Speed Drives Under Input Voltage Unbalance and Sag Conditions" IEEE Trans. Ind. Applicat, vol. 43, NO. 2, pp.495-504, Mar/Apr 2007

[15] Kevin Lee, Thomas M. Jahns, William E. Berkopec, and Thomas A. Lipo, " Closed-Form Analysis of Adjustable-Speed Drive Performance Under Input-Voltage Unbalance and Sag Conditions",.,vol.42, no. 3, pp. 733-741, May/June 2006

[16] G. Carpinelli, F. Iacovone, A. Russo, P. Varilone, and P. Verde, “Analytical modeling for harmonic analysis of line current of VSI-fed drives,” *IEEE Trans. Power Delivery*, vol. 19, no. 3, pp. 766–773, Apr. 2004.

[17] Kevin Lee, Giri Venkataramanan and Thomas M. Jahns," Source Current Harmonic Analysis of Adjustable Speed Drives Under Input Voltage Unbalance and Sag Conditions " *IEEE Trans. Power Delivery*, vol. 21, no. 2, pp.567-576, Apr 2006

[18] J. L. Duran-Gomez, P. N. Enjeti, and B. O. Woo, “Effect of voltage sags on adjustable-speed drives: A critical evaluation and an approach to improve performance,” *IEEE Trans. Ind. Applicat*., vol. 35, no. 6, pp. 1440–1449, Nov./Dec. 1999.

[19] N. Mohan, T. M. Undeland, and W. P. Robbins, *Power Electronics: Converters, Applications and Design*, 2nd ed. New York: Wiley, 1995.